Journal of Petroleum Research and Studies

Open Access
No. 41, December 2023, pp. 98-114

P- ISSN: 2220-5381
E- ISSN: 2710-1096

DOI: http://doi.org/10.52716/jprs.v13i4.750

Dissimilar Metal Welding by Resistance Spot Welding of 6061 Aluminum Alloy /AISI 1006 Steel Using Zn and Sn Coating

Ammar Y. Akkar[1*], Muhaed Alali[2]
University of Kufa, Faculty of Engineering, Materials Engineering Department, Najaf, Iraq
[*]Corresponding Author E-mail: ammaryasir.akar.35@gmail.com

Received 07/03/2023, Revised 19/04/2023, Accepted 25/04/2023, Published 12/12/2023

Abstract

This study was conducted to investigate the effect of welding parameters, and coating type on the weldability between 6061 aluminum alloy and AISI 1006 steel joints welded by the resistance spot welding technique. The mechanical properties, microstructure, and corrosion resistance were evaluated. The experimental tests used to evaluate the welded joint properties included a tensile shear test, microhardness test, microstructure examination, Energy dispersive X ray spectroscopy (EDS) analysis, and corrosion resistance test. However, Tin and zinc coating was utilized to improve the weldability of the joint. As a result, it was found that the maximum shear force for the welded joint without coating is 2.7 KN and increased to 4.24 KN when the use of coatings. For the microstructure characterization, a brazing-like joint was observed in the welded area that consists of a resolidified molten aluminum inside the weld nugget bonded with heat affected steel. Intermetallic compounds (IMC) of Fe - Al were detected at the joint interface by EDS analysis causing microcracks at the joint interface. Furthermore, Vickers microhardness varied across the joint due to the impact of welding heat and pressure on the base metals. Maximum hardness value was recorded in the thermo mechanical affected zone (TMAZ) at the steel side and the nugget zone consisted of aluminum with enhanced hardness due to the effect of Intermetallic compounds. Regarding the corrosion resistance, it was revealed that with increasing welding current, the corrosion rate increases due to the rise in the size of heat affected zones and nugget zone.

Keywords: Resistance Spot welding, Microhardness, Dissimilar metal welding, AISI 1006 steel, 6061 aluminum alloy, Tensile shear, Dissimilar welding, Zinc and tin coating, Corrosion.

Journal of Petroleum Research and Studies

Open Access
No. 41, December 2023, pp. 98-114

P- ISSN: 2220-5381
E- ISSN: 2710-1096

لحام المعادن المتباينة عن طريق اللحام النقطي بالمقاومة لسبائك الألومنيوم 6061 / الفولاذ AISI 1006 باستخدام طلاء الزنك والقصدير

الخلاصة:

أجريت هذه الدراسة لمعرفة تأثير متغيرات اللحام ونوع الطلاء على قابلية اللحام بين سبيكة الألومنيوم 6061 و الفولاذ AISI 1006 باستخدام تقنية لحام المقاومة النقطي. تضمنت الفحوصات المختبرية المستخدمة لتقييم خصائص الوصلات الملحومة اختبار قص الشد، واختبار الصلادة الدقيقة، وفحص البنية المجهرية، وتحليل مطيافية تشتت الطاقة بالأشعة السينية، واختبار مقاومة التآكل. تم استخدام طلاء القصدير و الزنك لتحسين قابلية اللحام للمفصل.

نتيجة لذلك، وجد أن أقصى قوة قص للمفصل الملحوم بدون طلاء تبلغ 2.7 كيلو نيوتن وتزداد إلى 4.24 كيلو نيوتن باستخدام الطلاءات. لوصف خصائص البنية المجهرية، لوحظ وجود لحام شبيه بلحام المونة في منطقة الربط التي تتكون من الألومنيوم المصهور المتصلب داخل منطقة اللحام المرتبطة بالمنطقة المتأثرة بالحرارة للفولاذ، تم الكشف عن المركبات البينية المعدنية من الفولاذ والالمنيوم في سطح المفصل عن طريق تحليل EDS مما تسبب في حدوث تشققات صغيرة في سطح المفصل. علاوة على ذلك، اختلفت صلادة فيكرز المايكروية عبر مفصل اللحام بسبب تأثير حرارة اللحام والضغط على المعادن الأساسية. تم تسجيل أقصى قيمة للصلادة في المنطقة التأثر الحراري الميكانيكي على جانب الفولاذ وتتكون منطقة اللحام من الألمنيوم مع صلادة محسنة بسبب تأثير المركبات البينية المعدنية. فيما يتعلق بمقاومة التآكل ، تم الكشف عن أنه مع زيادة تيار اللحام، يزداد معدل التآكل بسبب ارتفاع حجم المنطقة المتأثرة بالحرارة ومنطقة اللحام.

1. Introduction:

As a result of the expansion of industry, the joining of different types of metals now plays a significant role in a variety of different areas of manufacturing. Joining dissimilar metals may accomplish a combination of their benefits to improve properties and enhance the qualities of goods to better suit the demands of the chemical industry, the aerospace industry, and the automobile industry [1]. Weight reduction, environmental consideration, energy savings, superior performance, cost savings, and so on are only some of the reasons why dissimilar metal couplings are becoming more popular in industrial applications [2]. Welding aluminum to steel is an important process because the resulting products join of it combine the different properties of each component. For example, Al has a high thermal conductivity and a low density, while steel has a low thermal conductivity and a high tensile strength [3]. It is common knowledge that the physical, thermal, electrical, and mechanical properties of steel and aluminum alloys are significantly distinct from one another. Many brittle intermetallic compounds (IMC) are shown at fusion welded joints, which may quickly and readily result in the degradation of joint mechanical behavior [4]. Accordingly, it is difficult to obtain a reliable joint of steel to aluminum alloy by using conventional fusion welding. Fe and Al have limited solubility; thus, IMC formation is crucial for creating robust metallurgical bonding at the Al/Fe interface, however, the brittleness of the interface and the creation of voids and pores are two of the drawbacks associated with IMC due to a significant disparity in the thermal conductivities of the two metals. Electric arc welding, plasma

Open Access
No. 41, December 2023, pp. 98-114
P- ISSN: 2220-5381
E- ISSN: 2710-1096

sintering, high-energy beam welding, brazing, and soldering, resistance spot welding, and friction stir welding are all common ways to join pieces using heat. When compared to other joining methods, resistance spot welding (RSW) stands out because of its great efficiency, low cost, resilience, adaptability, and extensive applicability in similar metal joining in the automated manufacturing field [5]. In RSW, two or more pieces of metal are clamped between two copper electrodes. Through the electrode, pressure is put on the metal pieces, and then a high enough current flows to join the metal. The RSW consists of the following concatenation: Work-piece Setup, "Squeezing," Welding, and holding time. The welding parameters, which comprise "welding current, electrode pressure, squeeze time, and welding duration," are the primary factors that determine the quality of the welded joint [6]. The fundamental problem with dissimilar weld quality is the formation of brittle intermetallic phases, crack sensitivity, and corrosion prone. Researchers observed that reducing intermetallic compounds was a key element in improving the weld quality of dissimilar metal welds. Heat input control and filler metal alloying element selection may effectively minimize the quantity of intermetallic compounds as well as the growth of IMC layer thickness. The use of interlayers, cover plates, low heat input, and alloying components of filler metals are among the most significant attempts [7]. Interlayers such as Al0·5FeCoCrNi high entropy alloy (HEA) were applied to change the nature of the generated IMCs from Al_xFe_y to complicated IMCs in interlayer-free weldments. It was found that the latter prevented the Al-side of the weldments from cracking and the tensile shear strain of weldments manufactured with HEA interlayer was greater than that of an interlayer-free connection [8]. Cladding steel with an aluminum layer was also used to improve the resistance spot welding of aluminum to steel. It was observed that the development of a narrow Al/Fe intermetallic compound with a thickness of less than 3.5 m was caused by the metallurgical bonding that exists between the steel sheet and the Aluminium-clad layer. The cross-tension to the tensile-shear peak load ratio reached up to 0.5 at the highest tensile-shear peak load, which was an improvement compared to the results in the literature [9]. Therefore, this study aims to investigate the effect of the cover plate and metallic coating on weldability between AA6061 and AISI 1006 steel joints welded by the RSW technique using different conditions of welding current and time. The mechanical properties and corrosion resistance of the welded joints were evaluated and examined.

Open Access
No. 41, December 2023, pp. 98-114
P- ISSN: 2220-5381
E- ISSN: 2710-1096

2. Experimental work:

2.1 Metals Properties:

Two types of metal sheets were used, 6061 aluminum alloy sheets and AISI 1006 steel. For each material, two different thicknesses have been used 1.6 and 0.8 mm for aluminum and steel respectively. They have a chemical composition, as shown in Tables (1 and 2). Different thickness materials combined with the usage of a cover plate on the aluminum side were utilized to achieve heat balance and ensure that the two pieces being joined undergo a similar degree of heating to obtain a symmetrical weld nugget size on both materials as possible according to the following references: [Handbook, Miller. "Handbook for Resistance Spot Welding." Miller Electric Mfg. Co (2010)] and [Agashe, Soumitra, and H. Zhang. "Selection of schedules based on heat balance in resistance spot welding." Welding journal 82.7 (2003): 179-183].

Table (1): The chemical composition analysis of 6061 aluminum alloy[9].

Elements wt.%	Si%	Fe%	Cu%	Mn%	Mg%	Cr%	Zn%	Ti%	Al%
Standard	0.4-0.8	Max. 0.7	0.15-0.40	Max. 0.15	0.8-1.2	0.04-0.35	Max. 0.25	Max. 0.15	Balance
Obtained	0.703	0.477	0.251	0.131	0.909	0.193	0.0343	0.0757	97.2

Table (2): The chemical composition analysis of AISI 1006 steel

Elements wt%	C%	Si%	Mn%	P%	S%	Cr%	Mo%	Ni%	Fe%
Standard	0.08	-	0.25-0.4	0.04	0.05	-	-	-	-
Obtained	0.0726	0.0197	0.148	0.0185	0.0166	0.0421	0.0104	0.0302	Balance

* The standard chemical composition according to ASTM A568 standard.

2.2 Specimens Preparation:

The AA6061 and AISI 1006 sheets were cut into sheets with dimensions of (105×30 mm). These small sheets of dissimilar metals were welded together by RSW to produce a specimen for a tensile shear test according to EN ISO 14273. A cover plate of AISI 1006 steel with a thickness of 0.8 mm was used to perform the weld as shown in Figure (1).

Open Access
No. 41, December 2023, pp. 98-114
P- ISSN: 2220-5381
E- ISSN: 2710-1096

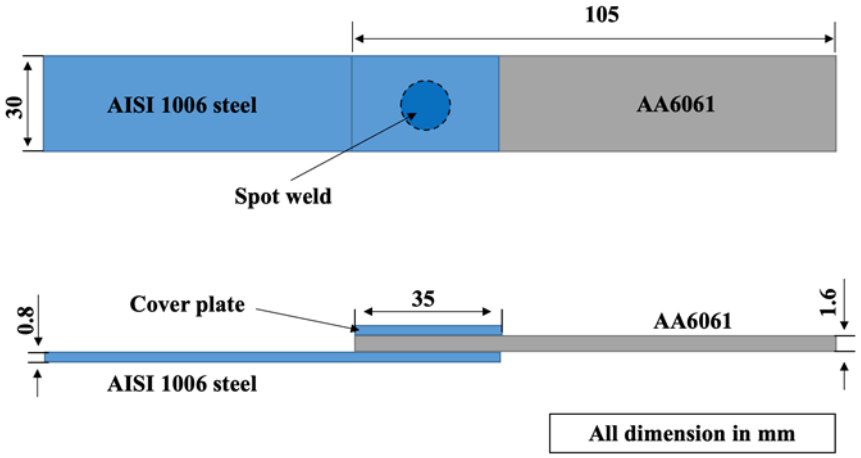

Fig. (1): The dimensions of the RSW tensile specimen according to EN ISO 14273 standard

2.3 Welding procedure:

Miller Electric's SSW-2020 equipment, made in the USA, was used to perform the weld. The details of this machine are shown in Table 3. Before welding, all dirt, and contamination were eliminated, and the specimens were entirely cleaned with acetone. The welding parameters and weldability were determined after several welding trials. The four spot welding parameters used in this investigation are welding current (KA), electrode force (KN), squeeze time (sec), and welding time (sec). The welding process was carried out with a constant electrode force of 12.2 N and a constant Squeeze time of 0.8 sec. The welding currents employed were (2,4,6 and 8) KA. Welding time was varied from 0.2 sec to 1 sec with a step of 0.2 sec as illustrated in Table (4).

Table (3) Welding Machine Details

Manufacturer	**Miller Electric Mfg .co. , USA**
Model	SSW-2020
Transformer	20 KVA
Power supply 50/60 HZ	(220-240) VAC
Electrode Face Diameter	5 mm
Electrode Force (min-max)	(11.69-19.48) N
Air Pressure (min-max)	(60-100) Psi
Max. Thickness	6 mm

Open Access
No. 41, December 2023, pp. 98-114
P- ISSN: 2220-5381
E- ISSN: 2710-1096

2.4 Coating procedure:

Both AA6061 aluminum alloy and AISI 1060 steel substrates received metallic zinc or tin coatings. Using electrolytic process. For the aluminum alloy sheets, any surface contaminates were removed then the sheets were rinsed with distilled water. After that, the sheets dip in nitric acid (HNO3) (50% by volume) for two minutes at room temperature followed by distilled water to rinse. Then zincate dips at 35 °C for two minutes. At this stage, double dipping has occasionally been proven to be beneficial. Regarding the coating of the steel sheets, the electroplating process was performed to coat AISI 1006 steel with tin. The sheet was cleaned to remove any surface contaminants. Then rinse using distilled water. This was followed by a dip in a diluted solution of hydrochloric acid (1:3) and then rinsing with distilled water. Finally, immerse the sheets for two minutes in a 50°C tin solution container. A summary of the weldment setup for coated and uncoated specimens is shown in Figure (2).

Table (4) Parameters for welding 6061 aluminum alloy to AISI 1006 steel

Specimen No.	Current (KA)	Time (sec)	Squeeze time (sec)	Electrode force (N)
1	2	0.2	0.8	12.2
2	4	0.2	0.8	12.2
3	6	0.2	0.8	12.2
4	8	0.2	0.8	12.2
5	2	0.4	0.8	12.2
6	4	0.4	0.8	12.2
7	6	0.4	0.8	12.2
8	8	0.4	0.8	12.2
9	2	0.6	0.8	12.2
10	4	0.6	0.8	12.2
11	6	0.6	0.8	12.2
12	8	0.6	0.8	12.2
13	2	0.8	0.8	12.2
14	4	0.8	0.8	12.2
15	6	0.8	0.8	12.2
16	8	0.8	0.8	12.2
17	4	1	0.8	12.2
18	8	1	0.8	12.2

Open Access
No. 41, December 2023, pp. 98-114
P- ISSN: 2220-5381
E- ISSN: 2710-1096

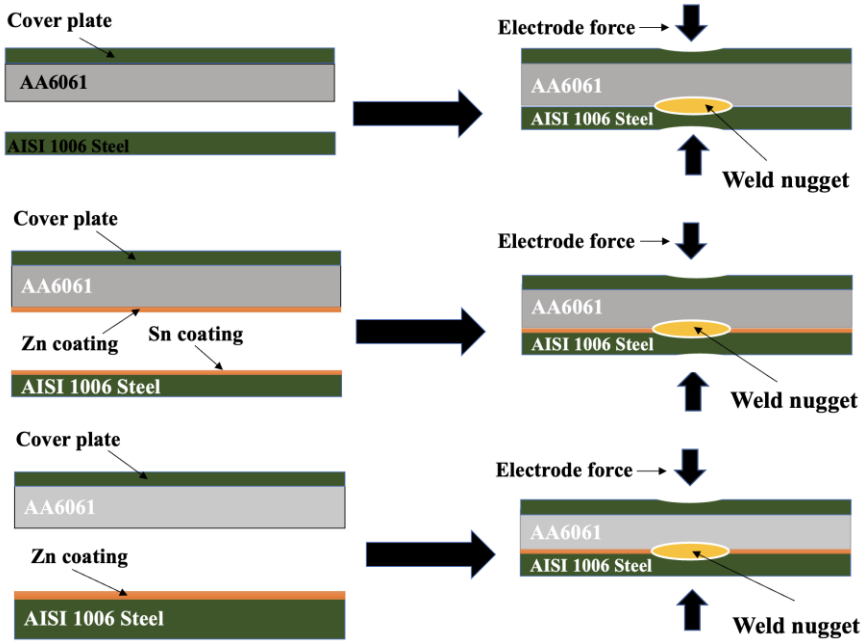

Fig. (2): Welding procedure for the specimens (a) as-weld. (b) coating both sides (c) coating one side

3. Experimental tests

3.1 Microstructure examination

For investigating the microstructure, the weldments were cut at the weld nugget cross-section using a wire-cutting machine to conduct metallographic analysis as shown in Figure (3). This was followed by the typical grinding and polishing processes. The grinding was conducted on the mounted specimens starting with sandpaper (400, 600, 800, 1000, 1200, 2000, and 2500) and then polished by fine cloth with the diamond paste of (3 μ) and Al_2O_3 solution. The specimens were then etched by immersing them in a solution of Nital, which consists of (2% mL HNO_3 and 98% mL Ethanol) for the carbon steel [10]. Etching did not conduct on aluminum alloy because the aluminum at the nugget area includes porosities that make the microstructure difficult to characterize. Furthermore, the important region to focus on in the weldment is the interaction zone between aluminum and steel. The microstructure was examined by an optical microscope and secondary electron microscope (SEM) equipped with EDS to analyze the microstructure and joint interface.

3.2 Tensile Shear Test

The tensile shear tests of the RSW joints were performed by Computer Controlled Electronic universal testing machine, model (UE3450) with a maximum capacity of (50) KN. Crossheads in

Open Access
No. 41, December 2023, pp. 98-114
P- ISSN: 2220-5381
E- ISSN: 2710-1096

this test were 1 mm/min. The test was conducted on the joint specimens that were cut according to EN ISO 14273 standard as presented in Figure (1).

3.3 Microhardness test

Vickers microhardness test was implemented for the cross-section of welded joints using (TH715, Digital Micro Vickers hardness tester, made in China). It is supplied with microscope lenses of a total magnification of 400 X. The Vickers measurements were taken in a contour line for different one-side regions of the spot weld cross section by using a 9.8 N load for low carbon steel and a 1.9 N load for aluminum alloy (due to the differences in materials' hardness). The test duration for each reading was reading 15 sec.

3.4 Corrosion test

The corrosion test was conducted to study the effect of the welding process on the corrosion behavior of welded joints in a corrosive media, especially with dissimilar metal joining. The corrosion behavior was evaluated by potential dynamic anodic polarization measurements (type is DY2321 potentiostats). The specimens were immersed in 3.5 wt% NaCl neutral solution. The purpose of choosing a 3.5 wt% NaCl neutral solution is to simulate the tropical marine atmosphere environment.

4. Results and Discussion

4.1 Shear Strength

The tensile-shear test was conducted to evaluate joint strength firstly for the specimens of as-welded coating condition that welded with 6 KA and 8 KA welding currents and 0.4, 0.6, and 1 sec welding times. Lower welding currents (2 and 4 KA) were not selected as a candidate for the tensile shear test because they produced a weak joint with all welding times with an interfacial failure mode as presented in Figure (3) (a). It was found that an increase in welding current and time above 8 KA and 0.6 sec caused an explosion defect at the joint region as illustrated in Figure (3) (b). For this reason, welding conditions of (6 KA, 0.6 sec) were chosen as the best welding conditions in terms of joint strength with the highest shear force of 2.7 KN Figure (4). For the specimens with coating conditions, the tensile shear tests were implemented for three coating conditions, namely, the as-welded joint, the Zn-coated steel to Al joint, and the Sn-coated steel to Zn-coated Al joint illustrated in Figure (2) using the best welding parameters (6 KA, 0.6 sec). The results showed that the shear force increased after applying the coating with 4.24 kN for the Sn-coated steel to the Zn-coated Al joint as shown in Figure (5). This increment might be attributed

Open Access
No. 41, December 2023, pp. 98-114
P- ISSN: 2220-5381
E- ISSN: 2710-1096

to the effect of coating since the interlayers at the joint interface was able to effectively reduce the thickness of the IMCs, which are a substantial contributor to the brittleness of the metallic junction since they typically display very poor plastic deformability and are considered a major cause of joint weakness [11]. It was reported that existing of an interlayer between aluminum and steel reduces the direct contact between the two materials and reduces the heat available at the interface region because the melting and evaporation of the coating layer consume some of the heat available for welding as well as decrease the thermal expansion mismatch between the substrates while the weld was being performed. It is worth mentioning that in all welding conditions, the fracture during the tensile shear test occurred at the interface area due to the reaction between aluminum and steel in this region and consequently the formation of intermetallic compounds. In pullout failure, a part of the aluminum remained joined with the steel sheet leaving the aluminum sheet with a hole as shown in Figure (3) (b).

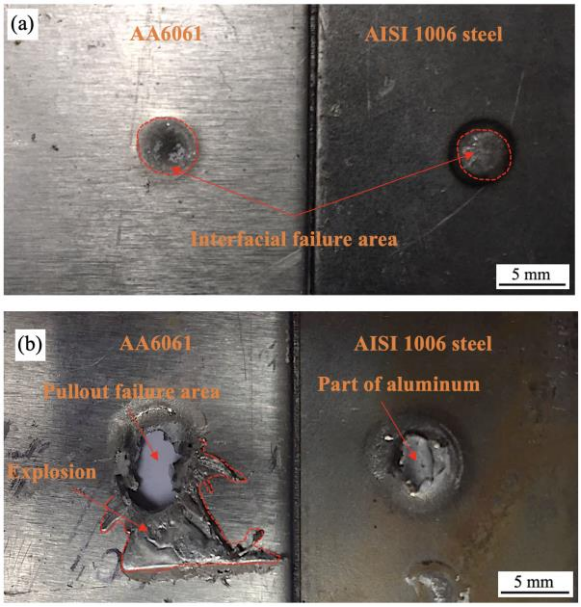

Fig. (3): Failure type for 6061 aluminum alloy /AISI 1006 steel joints without coating (a) Interfacial failure (b) Pullout failure

Open Access
No. 41, December 2023, pp. 98-114
P- ISSN: 2220-5381
E- ISSN: 2710-1096

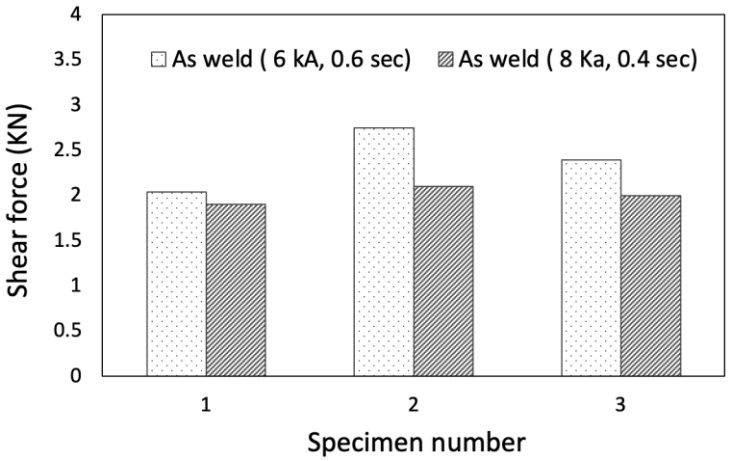

Fig. (4): Tensile shear force for 6061 aluminum alloy /AISI 1006 steel joints without coating

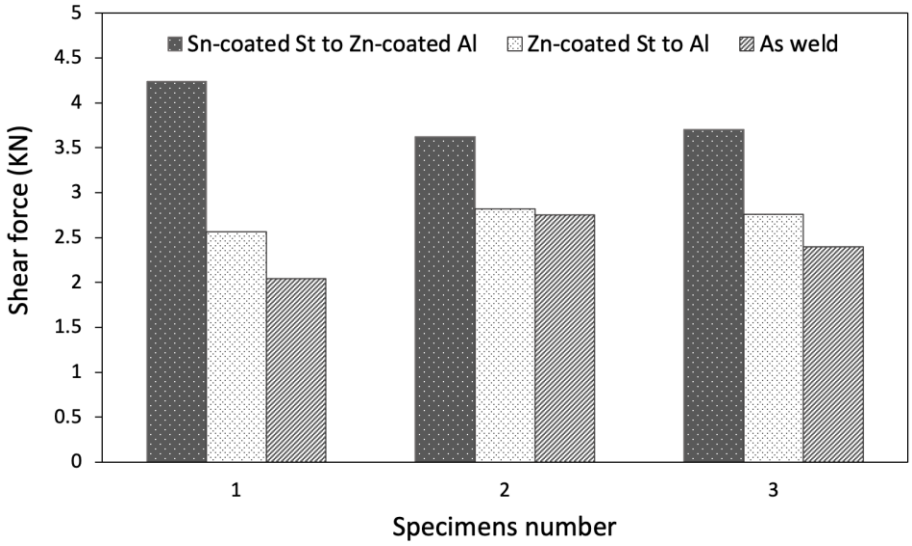

Fig. (5): Tensile shear force for 6061 aluminum alloy /AISI 1006 steel joints welded with (6KA, 0.6 Sec) and with different coating conditions

4.2 Microstructure examination and EDS analysis

The optical microscopy examination of the welded joint showed a brazing-like joint in the welded area that consists of a resolidified molten aluminum inside the weld nugget bonded with heat-affected steel as illustrated in Figure (6). The HAZ of steel can be classified into HAZ (Figures 6 c) and TMAZ (Figures 6 d). In the HAZ, the steel was exposed to the heat of welding while in TMAZ the steel was exposed to both electrode pressure and heat. The microstructure of BM Figure (6 e) and HAZ Figure (6 f) in steel were approximately similar and consisted of equiaxed ferrite and pearlite grains. While in the TMAZ the grains were deformed due to the application of pressure and heat during welding as presented in Figure (6 g). A further deep examination was carried out for the bonding area using SEM-EDS analysis as shown in Figure (6) which shows a clear joining

Open Access
No. 41, December 2023, pp. 98-114
P- ISSN: 2220-5381
E- ISSN: 2710-1096

between aluminum and steel. However, the EDS analysis indicated the existence of FeAl IMC despite the application of coating. The coating was detected by detecting a small amount of Zn the joint interface due to the evaporation of the coating layer during welding. which is found in a low percentage. Therefore, micro-cracks and porosities were detected in some joining areas near the interaction line between aluminum and steel due to the formation of IMC as presented in Figures (7, 8 and 9). This is proof that the failure always occurs at the interface area.

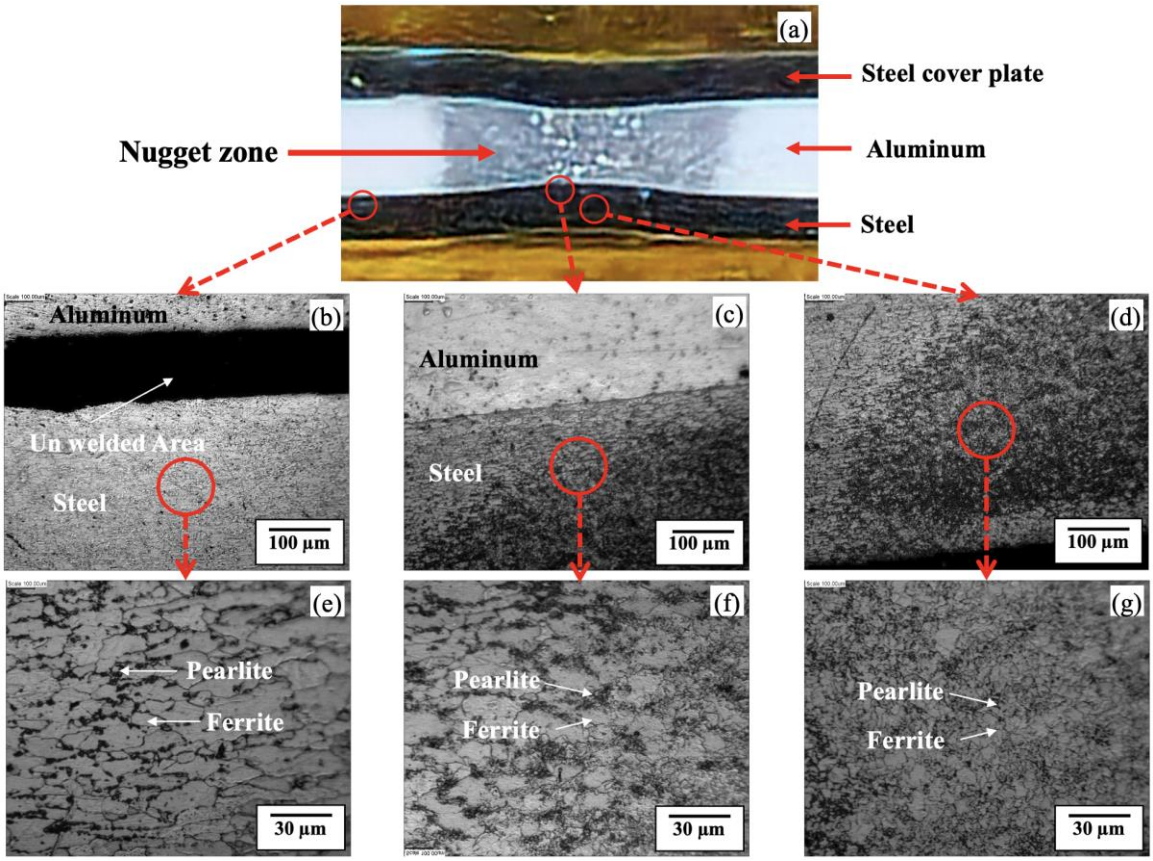

Fig. (6): Optical Microstructures of AISI 1006 steel side (a) Macro picture for the joint (b) BM (c) HAZ (d) TMAZ

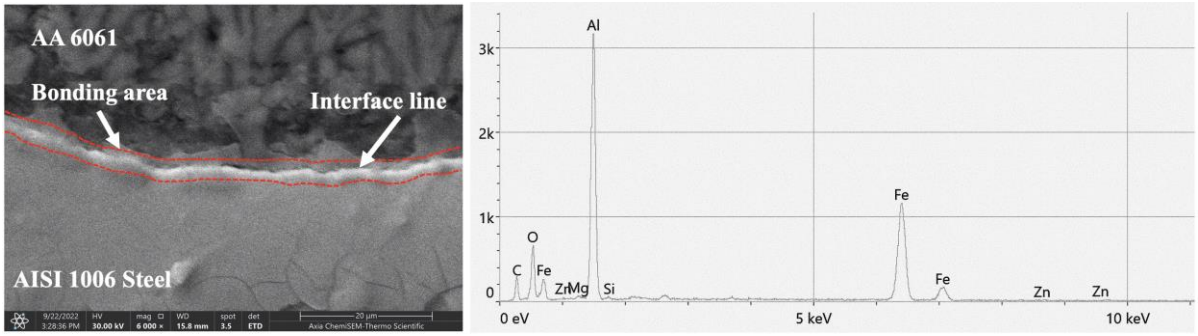

Fig. (7): SEM-EDX analysis of welded joints at 6KA, 0.6 Sec

Open Access
No. 41, December 2023, pp. 98-114
P- ISSN: 2220-5381
E- ISSN: 2710-1096

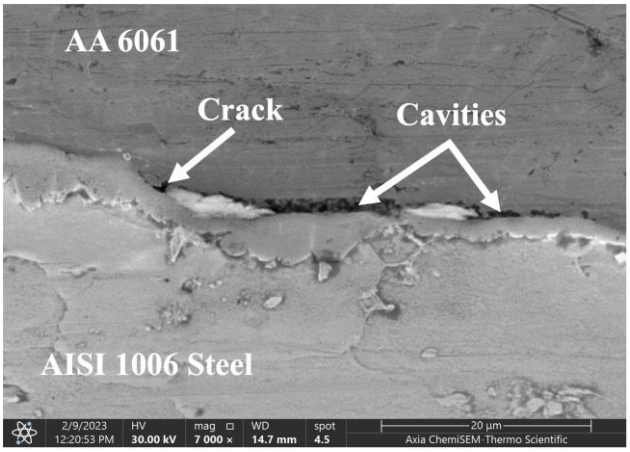

Fig. (8): SEM image at the Zn-coated steel to Al joint area at 6KA, 0.6 Sec

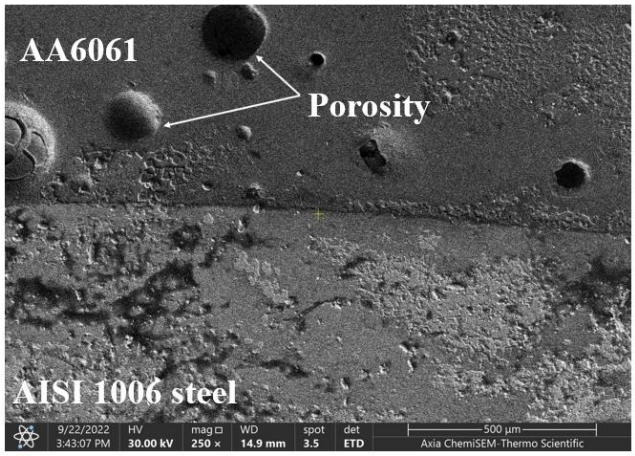

Fig. (9): SEM image shows porosity formation for joint Zn-coated steel to Al at Aluminium side6KA, 0.6 Sec

4.3 Microhardness

Figure (10) shows the results of the average Vickers microhardness value along a cross-section of 6061 aluminum alloy / AISI 1006 steel resistance spot welded joints at different coating types. The tests covered the base metal (BM), heat affected zone (HAZ), thermomechanical affected zone (TMAZ), and nugget zone, represented by six circles shown in Figure (7). The joint coating conditions are classified as: without coating (as-welded), tin-coated steel with zinc-coated aluminum, and zinc-coated steel with aluminum. The hardness of the 6061-aluminum alloy and AISI 1006 steel in unaffected (BM) recorded 42 HV for 6061 aluminum alloy (region 1) and 120 HV for AISI 1006 steel (region 2). Further toward the nugget zone, the hardness results showed a reduction in the HAZ of 6061 aluminum alloy (region 3), which might be attributed to the dissolution of strengthening precipitates [Reference]. While in the HAZ of steel (region 4), the

Open Access
No. 41, December 2023, pp. 98-114
P- ISSN: 2220-5381
E- ISSN: 2710-1096

microhardness values were close to the BM because it was exposed to relatively low heat input due to the localized and fast heating of the RSW process, and the microstructure of the heat-affected zone Figure (5 c and f) did not show a significant change compared to the microstructure of the BM Figure (5 b and e). In TMAZ (region 5) microhardness was significantly higher than that of HAZ and BM because of the influence of heat and pressure resulting from the RSW electrode applied in this area, which produced deformed small-size grains (Figure 5 d and g) with enhanced hardness. In the nugget zone (region 6), which consisted of aluminum, the average microhardness was higher than the BM and HAZ. This increment in hardness in the nugget zone can be accredited to the presence of IMCs of Fe-Al; these IMCs are brittle in nature which induces the hardness enhancement in the nugget zone.

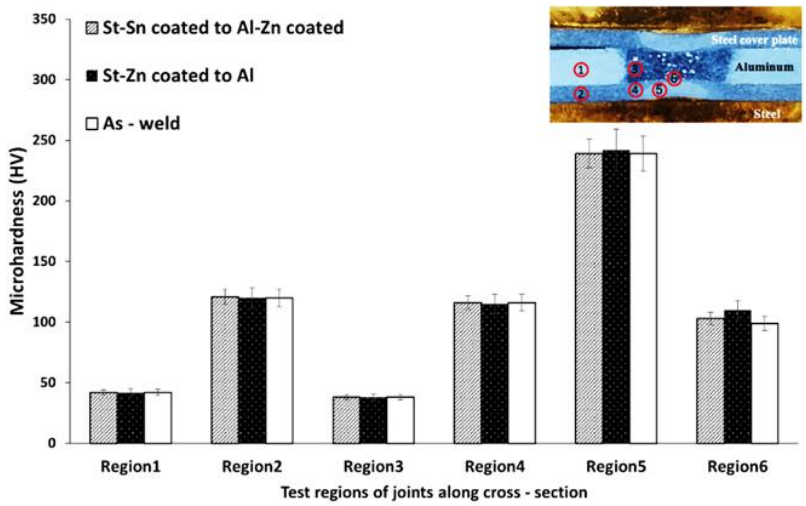

Fig. (10): Results of Vickers hardness of cross-section of AISI 1006 Steel /6061 aluminum alloy joint at the best welding condition

4.4 Corrosion behavior

Linear polarization was used to calculate corrosion potential (E corr.) and corrosion current density (I corr.) through the point of intersecting both Tafel lines (Ecorr. and Icorr.) that makes possible for the estimation of the corrosion current density by the extrapolation of the Tafel slopes with corrosion potential. Three specimens of Sn-coated steel to Zn-coated Al were tested under different welding currents (4KA, 6KA, and 8KA) with a constant weld time of 0.6 sec. The specimens were immersed in 3.5 wt% NaCl neutral solution. It was noticed that when the welding current increased, the corrosion current also increased, which also means an increase in the corrosion rate as shown in Figure (11) and can also be seen in the anodic and cathodic polarization curves shown in Figure (12). This increment in corrosion rate might be attributed to the increase of the HAZ,

Open Access
No. 41, December 2023, pp. 98-114
P- ISSN: 2220-5381
E- ISSN: 2710-1096

TMAZ, and nugget zone size as presented in Figure (13). The HAZs and nugget zone have a change in their microstructure that might negatively affect the corrosion resistance of the joint.

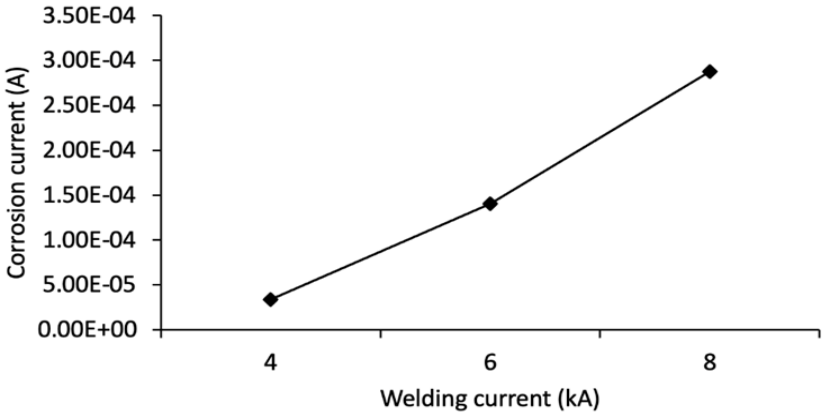

Fig. (11): Relationship between corrosion current and weld current.

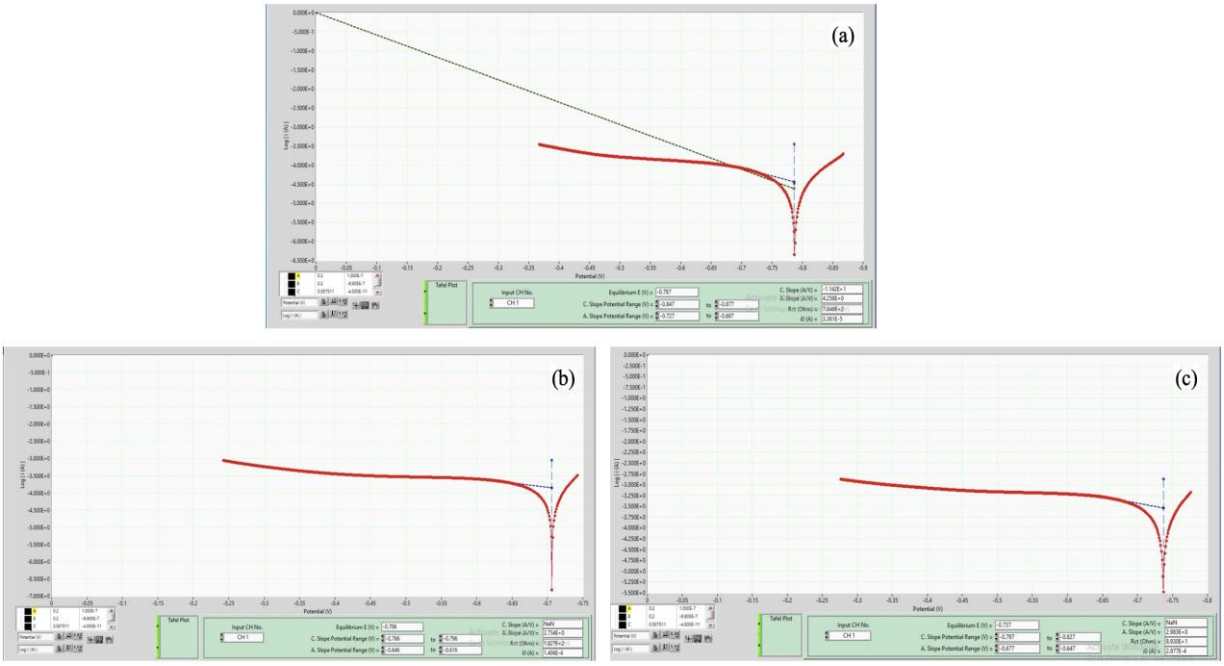

Fig. (12): Polarization Curves for Dissimilar AA6061/ AISI 1006 steel joint in 3.5% NaCl Solution at (a) 4KA,0.6 sec (b) 6KA, 0.6 sec (c) 8KA, 0.6 sec

Open Access
No. 41, December 2023, pp. 98-114
P- ISSN: 2220-5381
E- ISSN: 2710-1096

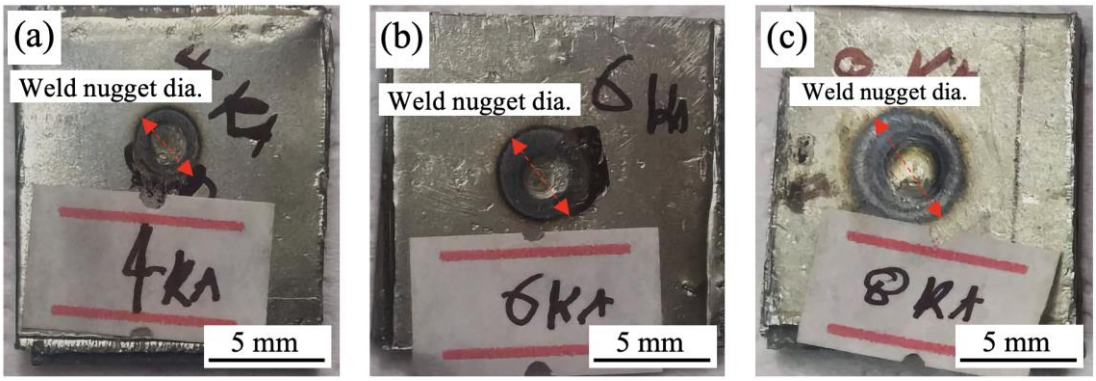

Fig. (13): Weld nugget diameters of RSW joints welded at different welding currents a) 4KA,0.6 sec (b) 6KA, 0.6 sec (c) 8KA, 0.6 sec

5. Conclusions

The important conclusions of this research are listed below:

1. The low welding current produces welded joints with weak interfacial failure type. Increasing welding current produces a stronger weld with pullout failure type. Further increase in welding current caused an explosion defect at the joint area.
2. Maximum shear force obtained for as-welded joints is 2.7 kN. Utilizing the coating raises the maximum shear force obtained to 4.24 kN with a 57% increase in maximum shear load.
3. The weld nugget was made from resolidified aluminum connected by a brazing mechanism to the steel HAZ.
4. On the steel side, a mixture of ferrite and pearlite is observed in the BM, HAZ, and TMAZ. With finer and deformed grains in the TMAZ compared to BM and HAZ.
5. The TMAZ region of steel has the maximum value of Vickers hardness compared to other regions in the welded joint.
6. On the aluminum side, the HAZ has a lower Vickers hardness than the BM, and the nugget zone consisted of aluminum with enhanced hardness due to the effect of IMCs.
7. Increasing welding current attributes in increasing the corrosion rate due to the increase in the size of HAZ and nugget zone.

Open Access
No. 41, December 2023, pp. 98-114
P- ISSN: 2220-5381
E- ISSN: 2710-1096

References

[1] Y. Fang, X. Jiang, D. Mo, D. Zhu, and Z. Luo, "A review on dissimilar metals' welding methods and mechanisms with interlayer", *Int. J. Adv. Manuf. Technol.*, vol. 102, no. 9–12, pp. 2845–2863, Jun. 2019. https://doi.org/10.1007/s00170-019-03353-6

[2] Shao, L., Shi, Y., Huang, J. K., & Wu, S. J, "Effect of joining parameters on microstructure of dissimilar metal joints between aluminum and galvanized steel", *Mater. Des.*, vol. 66, pp. 453–458, 2014. https://doi.org/10.1016/j.matdes.2014.06.026

[3] M. Yilmaz, M. Çöl, and M. Acet, "Interface properties of aluminum/steel friction-welded components", *Mater. Charact.*, vol. 49, no. 5, pp. 421–429, Dec. 2002. https://doi.org/10.1016/S1044-5803(03)00051-2

[4] W. H. Zhang, X. M. Qiu, D. Q. Sun, and L. J. Han, "Effects of resistance spot welding parameters on microstructures and mechanical properties of dissimilar material joints of galvanised high strength steel and aluminium alloy", *Sci. Technol. Weld. Join.*, vol. 16, no. 2, pp. 153–161, Feb. 2011. https://doi.org/10.1179/1362171810Y.0000000009

[5] C. Chen, L. Kong, M. Wang, A. S. Haselhuhn, D. R. Sigler, H. P. Wang, & B. E. Carlson, "The robustness of Al-steel resistance spot welding process", *J. Manuf. Process.*, vol. 43, pp. 300–310, Jul. 2019. https://doi.org/10.1016/j.jmapro.2019.02.030

[6] S. M. Hassoni, O. S. Barrak, M. I. Ismail, & S. K. Hussein, "Effect of Welding Parameters of Resistance Spot Welding on Mechanical Properties and Corrosion Resistance of 316L", *Mater. Res.*, vol. 25, 2022. https://doi.org/10.1590/1980-5373-MR-2021-0117

[7] M. Abdul Karim and Y.-D. Park, "A Review on Welding of Dissimilar Metals in Car Body Manufacturing", journal of Welding and Joining, vol. 38, no. 1, pp. 8–23, Feb. 2020. https://doi.org/10.5781/JWJ.2020.38.1.1

[8] H. Azhari-Saray, M. Sarkari-Khorrami, A. Nademi-Babahadi, & S. F. Kashani-Bozorg, "Dissimilar resistance spot welding of 6061-T6 aluminum alloy/St-12 carbon steel using a high entropy alloy interlayer", *Intermetallics*, vol. 124, 2020. https://doi.org/10.1016/j.intermet.2020.106876

[9] R. K. Prabakaran, A. Naveen Sait, and V. Sentilkumar, "Synthesis and characteristization of high entropy alloy (CrMnFeNiCu) reinforced 6061 aluminum alloy aluminium matrix composite", *J. Mech. Mechan. Eng*, vol. 21, no. 4, pp. 823-832., 2017.

[10] M. H. Abass, A. N. Abood, M. Alali, S. K. Hussein, and S. A. Nawi, "Mechanical Properties

Open Access
No. 41, December 2023, pp. 98-114
P- ISSN: 2220-5381
E- ISSN: 2710-1096

And Microstructure Evolution in Arc Stud Welding Joints of AISI 1020 with AISI 316L and AISI 304", *Metallogr. Microstruct. Anal.*, vol. 10, no. 3, pp. 321–333, Jun. 2021. https://doi.org/10.1007/s13632-021-00744-8

[11] Y. Ma, H. Dong, Y. Wang, G. Yang, Y. Xia, P. Li, X. Hao, J. Yang, B. Guo, H. Ji, & M. Lei, "Effect of Zn coating on microstructure and corrosion behavior of dissimilar joints between aluminum alloy and steel by refilled friction stir spot welding", *Metals (Basel).*, vol. 52, no. 1, pp. 85–102, Jan. 2022. https://doi.org/10.1007/s10800-021-01610-9